2012 American Control Conference
Fairmont Queen Elizabeth, Montréal, Canada
June 27-June 29, 2012

Slow-fast decomposition of an inertialess flow of viscoelastic fluids

Binh K. Lieu and Mihailo R. Jovanović

***Abstract*— We study frequency responses of an inertialess two-dimensional channel flow of viscoelastic fluids. By rewriting the evolution equations in terms of low-pass filtered versions of the stream function, we show that strongly-elastic flows can be brought into a standard singularly perturbed form that exhibits a slow-fast decomposition. In high-Weissenberg number regime, which is notoriously difficult to study numerically, we demonstrate that the frequency responses are reliably captured by the dynamics of the fast subsystem. We use numerical computations to validate our theoretical findings and to illustrate that our formulation does not suffer from spurious numerical instabilities.**

***Index Terms*— Energy amplification; frequency responses; singular perturbation analysis; viscoelastic fluids.**

I. Introduction

Viscoelastic fluids, such as polymer solutions and molten plastics, are often encountered in industrial and biological flows. Their micro-scale properties are significantly more complex than those in Newtonian fluids. Recent experiments have shown that fluids containing long polymer chains may become turbulent even at low flow rates [1]–[3]. This is in contrast to Newtonian fluids that become turbulent only at high speeds. Our recent work suggests that velocity and stress fluctuations in viscoelastic fluids can exhibit large amplification even in the absence of inertia [4]–[8].

In this paper, we consider a two-dimensional inertialess shear-driven flow of viscoelastic fluids. We identify the slow-fast system decomposition and utilize singular perturbation analysis to show that, in strongly elastic flows, the frequency responses are captured by the fast subsystem. The evolution representation that we determine facilitates reliable computation of the frequency responses in the high-Weissenberg number regime, which is known to exhibit spurious numerical instabilities [9], [10].

Our presentation is organized as follows. In Section II, we present the governing equations. In Section III, we discuss the method for transforming the governing equations into an evolution representation where the states are determined by the filtered versions of the stream function. In Section IV, we show that the evolution model admits a standard singularly perturbed form, thereby identifying the slow-fast decomposition of the inertialess channel flow. In Section V, we compute the frequency responses to validate our theoretical results. We conclude with a summary of our developments and a highlight of remaining challenges in Section VI.

Financial support from the National Science Foundation under CAREER Award CMMI-06-44793 and from the University of Minnesota Doctoral Dissertation Fellowship is gratefully acknowledged.

B. K. Lieu and M. R. Jovanović are with the Department of Electrical and Computer Engineering, University of Minnesota, Minneapolis, MN 55455, USA (e-mails: lieux006@umn.edu, mihailo@umn.edu).

II. Governing equations

The momentum, continuity, and constitutive equations for a two-dimensional incompressible channel flow of viscoelastic fluids, with geometry shown in Fig. 1, are given by

$$Re\,\dot{\mathbf{V}} = We\Big(\beta\,\boldsymbol{\nabla}^2\mathbf{V} - \boldsymbol{\nabla}P - Re\,\mathbf{V}\cdot\boldsymbol{\nabla}\mathbf{V} + (1-\beta)\,\boldsymbol{\nabla}\cdot\mathbf{T}\Big), \tag{1a}$$

$$0 = \nabla\cdot\mathbf{V}, \tag{1b}$$

$$\dot{\mathbf{T}} = \boldsymbol{\nabla}\mathbf{V} + (\boldsymbol{\nabla}\mathbf{V})^T - \mathbf{T} + We\Big(\mathbf{T}\cdot\boldsymbol{\nabla}\mathbf{V} + (\mathbf{T}\cdot\boldsymbol{\nabla}\mathbf{V})^T - \mathbf{V}\cdot\boldsymbol{\nabla}\mathbf{T}\Big). \tag{1c}$$

Here, dot denotes partial derivative with respect to time t, $\mathbf{V}$ is the velocity vector, P is pressure, $\mathbf{T}$ is the polymer stress tensor, $\boldsymbol{\nabla}$ is the gradient, and $\boldsymbol{\nabla}^2$ is the Laplacian. System (1) has been non-dimensionalized by scaling length with the channel half-height L, time with the fluid relaxation time λ, velocity with the largest base flow velocity U_0, polymer stresses with $\eta_p U_0/L$, and pressure with $(\eta_s+\eta_p)\,U_0/L$, where η_s and η_p are the solvent and polymer viscosities. The key parameters in (1) are: the viscosity ratio, $\beta = \eta_s/(\eta_s+\eta_p)$; the Weissenberg number, $We = \lambda U_0/L$, which is the ratio of the fluid relaxation time to the characteristic flow time L/U_0; and the Reynolds number, $Re = \rho U_0 L/(\eta_s+\eta_p)$, which represents the ratio of inertial to viscous forces, where ρ is the fluid density.

The momentum (1a) and continuity (1b) equations describe the motion of an incompressible viscoelastic fluid. For given $\mathbf{T}$, the pressure adjusts itself so that velocity satisfies the continuity equation (1b). The constitutive equation (1c) is given for an Oldroyd-B fluid and it captures the influence of velocity gradients on the evolution of polymer stress fluctuations. This equation is obtained for dilute polymer solutions in which each polymer molecule is modeled by two spherical beads connected by a linear spring [11].

In shear driven flow, the steady-state solution of (1) is given by

$$\bar{\mathbf{v}} = \begin{bmatrix} y \\ 0 \end{bmatrix}, \quad \bar{\boldsymbol{\tau}} = \begin{bmatrix} \bar{\tau}_{11} & \bar{\tau}_{12} \\ \bar{\tau}_{12} & \bar{\tau}_{22} \end{bmatrix} = \begin{bmatrix} 2We & 1 \\ 1 & 0 \end{bmatrix}.$$

Recent experiments have shown that flows of viscoelastic fluids may become turbulent (i.e., undergo a transition to a time-dependent disordered flow state) even when inertial forces are considerably weaker than viscous forces [1]–[3]. Hence, in this work, we consider flows in the absence of

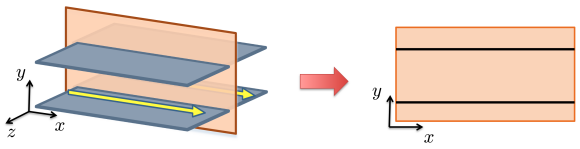

Fig. 1. Channel flow geometry. We consider the dynamics of two-dimensional flow fluctuations in the (x, y)-plane.

inertia, i.e. at $Re = 0$. In this case, the linearized equations governing the dynamics of fluctuations around the base flow $(\bar{\mathbf{v}}, \bar{\boldsymbol{\tau}})$ are given by

$$0 = -\boldsymbol{\nabla} p + (1-\beta)\boldsymbol{\nabla}\cdot\boldsymbol{\tau} + \beta\boldsymbol{\nabla}^2\mathbf{v} + \mathbf{d}, \tag{2a}$$

$$0 = \boldsymbol{\nabla}\cdot\mathbf{v}, \tag{2b}$$

$$\dot{\boldsymbol{\tau}} = \boldsymbol{\nabla}\mathbf{v} + (\boldsymbol{\nabla}\mathbf{v})^T - \boldsymbol{\tau} + We\,(\boldsymbol{\tau}\cdot\boldsymbol{\nabla}\bar{\mathbf{v}} + \bar{\boldsymbol{\tau}}\cdot\boldsymbol{\nabla}\mathbf{v} + (\bar{\boldsymbol{\tau}}\cdot\boldsymbol{\nabla}\mathbf{v})^T + (\boldsymbol{\tau}\cdot\boldsymbol{\nabla}\bar{\mathbf{v}})^T - \mathbf{v}\cdot\boldsymbol{\nabla}\bar{\boldsymbol{\tau}} - \bar{\mathbf{v}}\cdot\boldsymbol{\nabla}\boldsymbol{\tau}), \tag{2c}$$

where $\mathbf{v} = \begin{bmatrix} u & v \end{bmatrix}^T$, p, and $\boldsymbol{\tau}$ are, respectively, the velocity vector, pressure, and polymer stress tensor fluctuations with u and v denoting the streamwise and wall-normal velocities. System (2) is driven by the spatially distributed and temporally varying body force fluctuations $\mathbf{d} = \begin{bmatrix} d_1 & d_2 \end{bmatrix}^T$ with d_1 and d_2 representing the forcing in the streamwise (x) and wall-normal (y) directions, respectively.

The pressure can be eliminated from the equations by expressing the velocity fluctuations in terms of the stream function ψ,

$$u = \partial_y\psi, \quad v = -\partial_x\psi.$$

Furthermore, by rearranging the polymer stresses

$$\boldsymbol{\phi} = \begin{bmatrix} \phi_1 & \phi_2 & \phi_3 \end{bmatrix}^T = \begin{bmatrix} \tau_{22} & \tau_{12} & \tau_{11} \end{bmatrix}^T,$$

and by applying the Fourier transform in the x-direction we arrive at a set of PDEs in $y \in [-1, 1]$ and t parameterized by the wave-number k_x,

$$\dot{\phi}_1 = -f(y)\,\phi_1 + F_{1\psi}\,\psi, \tag{3a}$$

$$\dot{\phi}_2 = -f(y)\,\phi_2 + We\,\phi_1 + F_{2\psi}\,\psi, \tag{3b}$$

$$\dot{\phi}_3 = -f(y)\,\phi_3 + 2\,We\,\phi_2 + F_{3\psi}\,\psi, \tag{3c}$$

$$\Delta^2\psi = \frac{1-\beta}{\beta}\left(F_{\psi 1}\,\phi_1 + F_{\psi 2}\,\phi_2 + F_{\psi 3}\,\phi_3\right) + \frac{1}{\beta}\left(-\partial_y\,d_1 + \mathrm{j}k_x\,d_2\right), \tag{3d}$$

where j is the imaginary unit and

$$\begin{aligned} &F_{1\psi} = 2\left(We\,k_x^2 - \mathrm{j}k_x\partial_y\right),\ F_{2\psi} = \partial_{yy} + (1+2\,We^2)\,k_x^2,\\ &F_{3\psi} = 2\,\mathrm{j}k_x\left(1+2\,We^2\right)\partial_y + 2\,We\,\partial_{yy},\\ &F_{\psi 1} = \mathrm{j}k_x,\ F_{\psi 2} = -\left(\partial_{yy} + k_x^2\right),\ F_{\psi 3} = -\mathrm{j}k_x,\\ &f(y) = 1 + We\,\mathrm{j}k_x\,y,\ \Delta^2 = \partial_{yyyy} - 2\,k_x^2\,\partial_{yy} + k_x^4. \end{aligned} \tag{4}$$

For notational convenience, we have suppressed the dependence of $\{\phi_i, \psi, d_j\}$ on $(k_x, y, t; \beta, We)$, which is a convention we adopt from now on.

The boundary conditions on the stream function are induced by the no-slip and no-penetration criteria on velocity fluctuations and they are given by

$$\psi(k_x, y = \pm 1, t) = \partial_y\psi(k_x, y = \pm 1, t) = 0.$$

Note that the kinetic energy density of the velocity fluctuations is determined by the L_2-norm of $\mathbf{v} = \begin{bmatrix} u & v \end{bmatrix}^T$

$$E(k_x, t) = \langle u, u\rangle + \langle v, v\rangle = \langle\psi, -\Delta\psi\rangle = \langle\psi, \psi\rangle_e, \tag{5}$$

where $\Delta = \partial_{yy} - k_x^2$ and $\langle\cdot,\cdot\rangle$ denotes the standard $L_2[-1, 1]$ inner product

$$\langle u, u\rangle = \int_{-1}^{1} u^*(k_x, y, t)\,u(k_x, y, t)\,\mathrm{d}y.$$

The inner product $\langle\cdot,\cdot\rangle_e$ in (5) along with the boundary conditions on ψ determines the Hilbert space that the stream function belongs to

$$\mathbb{H} := \{\psi \in L_2[-1, 1];\ \partial_{yy}\psi \in L_2[-1, 1],\ \psi(\pm 1) = 0\}. \tag{6}$$

On the other hand, the elastic energy of the polymer stresses is not quantified by an L_2-norm and there are no boundary conditions on the components of $\boldsymbol{\tau}$. Consequently, it is difficult to determine the appropriate Hilbert space for the polymer stress fluctuations. Furthermore, it is well known that the set of equations (3) exhibits spurious numerical instabilities [9], [10] which is an obstacle to conducting high-fidelity simulations of viscoelastic fluids.

In this work, we show how (3) can be brought into an evolution representation that is amenable to both analytical and computational developments. In addition, we demonstrate that the inertialess channel flow can be decomposed into slow and fast subsystems. At high-Weissenberg numbers, singular perturbations reveal that the system's dynamics are captured by the dynamics of the fast subsystem. Furthermore, we illustrate that the computation of the frequency responses does not exhibit any numerical instabilities upon grid refinement. This suggests that the inherent presence of two-time scales in the system's dynamics may represent one source of numerical difficulties. Full nonlinear simulations may thus not be able to capture the response of the fast subsystem correctly, and, as we show, this subsystem contributes significantly to the fluctuation's energy.

III. Evolution Equations and Low-Pass Versions of the Stream Functions

In what follows, we show how to transform (3) into an evolution representation where the state variables are filtered versions of the stream function. This new representation of system (2) has two major advantages:

- the state space is a well-defined Hilbert space;
- the evolution equations are posed in a form that is well-suited for analysis and computations.

We begin by applying the temporal Fourier transform with zero initial conditions on (3a) – (3c)

$$\phi_1 \;=\; \frac{1}{\mathrm{j}\omega + f(y)}\, F_{1\psi}\, \psi, \tag{7a}$$

$$\phi_2 \;=\; \frac{1}{\mathrm{j}\omega + f(y)}\, (We\, \phi_1 \;+\; F_{2\psi}\, \psi)\,, \tag{7b}$$

$$\phi_3 \;=\; \frac{1}{\mathrm{j}\omega + f(y)}\, (2\, We\, \phi_2 \;+\; F_{3\psi}\, \psi)\,, \tag{7c}$$

where ω is the temporal frequency. Let us introduce the following low-pass versions of the stream function,

$$\xi_1 \;=\; \frac{1}{\mathrm{j}\omega + f(y)}\, \psi, \tag{8a}$$

$$\xi_2 \;=\; \frac{1}{(\mathrm{j}\omega + f(y))^2}\, \psi \;=\; \frac{1}{\mathrm{j}\omega + f(y)}\, \xi_1, \tag{8b}$$

$$\xi_3 \;=\; \frac{1}{(\mathrm{j}\omega + f(y))^3}\, \psi \;=\; \frac{1}{\mathrm{j}\omega + f(y)}\, \xi_2, \tag{8c}$$

which will be used as state variables in the evolution representation. We first consider (7a)

$$\phi_1 = \frac{1}{\mathrm{j}\omega + f(y)}\, F_{1\psi}\, \psi \;=\; \frac{2\, We\, k_x^2}{\mathrm{j}\omega + f(y)}\, \psi \;-\; \frac{2\, \mathrm{j} k_x}{\mathrm{j}\omega + f(y)}\, \psi', \tag{9}$$

where $\psi'(y) = \partial\psi/\partial y$. Since

$$\begin{aligned} \frac{1}{\mathrm{j}\omega + f(y)}\, \psi' \;&=\; \partial_y \left[\frac{1}{\mathrm{j}\omega + f(y)}\, \psi \right] \;+\; \frac{f'(y)}{(\mathrm{j}\omega + f(y))^2}\, \psi \\ &=\; \partial_y\, \xi_1 \;+\; f'(y)\, \xi_2 \\ &=\; \partial_y\, \xi_1 \;+\; We\, \mathrm{j} k_x\, \xi_2, \end{aligned}$$

we can rewrite (9) in terms of ξ_1 and ξ_2

$$\phi_1 \;=\; 2\left(We\, k_x^2 \;-\; \mathrm{j} k_x\, \partial_y\right) \xi_1 + 2\, We\, k_x^2\, \xi_2. \tag{10}$$

Using similar procedure, we can express ϕ_2 and ϕ_3 in terms of ξ_1, ξ_2, and ξ_3,

$$\begin{aligned} \phi_2 \;=\; &\left(\partial_{yy} \;+\; \left(1 \;+\; 2\, We^2\right) k_x^2\right) \xi_1 \\ &+\; 2\, We^2\, k_x^2\, \xi_2 \;+\; 2\, We^2\, k_x^2\, \xi_3, \end{aligned} \tag{11a}$$

$$\begin{aligned} \phi_3 \;=\; &\left(2\, We\, \partial_{yy} \;+\; 2\left(1 \;+\; 2\, We^2\right) \mathrm{j} k_x\, \partial_y\right) \xi_1 \\ &+\; \left(2\, We\, \partial_{yy} \;+\; 4\, We^2\, \mathrm{j} k_x\, \partial_y\right) \xi_2 \;+\; 4\, We^2\, \mathrm{j} k_x\, \partial_y\, \xi_3. \end{aligned} \tag{11b}$$

We can now obtain an evolution representation of system (3) by letting

$$\boldsymbol{\xi} \;=\; \left[\; \xi_1 \quad \xi_2 \quad \xi_3 \;\right]^T,$$

be the state and by applying the inverse temporal Fourier transform to (8)

$$\begin{aligned} \xi_1 \;&=\; \frac{1}{\mathrm{j}\omega + f(y)}\, \psi \quad\Rightarrow\quad \dot{\xi}_1 \;=\; -f(y)\, \xi_1 + \psi, \\ \xi_2 \;&=\; \frac{1}{\mathrm{j}\omega + f(y)}\, \xi_1 \quad\Rightarrow\quad \dot{\xi}_2 \;=\; -f(y)\, \xi_2 + \xi_1, \\ \xi_3 \;&=\; \frac{1}{\mathrm{j}\omega + f(y)}\, \xi_2 \quad\Rightarrow\quad \dot{\xi}_3 \;=\; -f(y)\, \xi_3 + \xi_2. \end{aligned}$$

Furthermore, substitution of (10) and (11) into (3d) yields an expression for the stream function in terms of $\boldsymbol{\xi}$.

In summary, the evolution model is given by

$$\dot{\boldsymbol{\xi}}(k_x, y, t) \;=\; \mathcal{A}\, \boldsymbol{\xi}(k_x, y, t) \;+\; \mathcal{B}\, \psi(k_x, y, t), \tag{12a}$$

$$\psi(k_x, y, t) \;=\; We^2\, \mathcal{C}_\psi\, \boldsymbol{\xi}(k_x, y, t) \;+\; \mathcal{D}\, \mathbf{d}(k_x, y, t), \tag{12b}$$

where

$$\mathcal{A} = \begin{bmatrix} -f(y) & 0 & 0 \\ I & -f(y) & 0 \\ 0 & I & -f(y) \end{bmatrix},\; \mathcal{B} \;=\; \begin{bmatrix} I \\ 0 \\ 0 \end{bmatrix},$$

$$\mathcal{C}_\psi = \left[\; \mathcal{C}_{\psi 1} \quad \mathcal{C}_{\psi 2} \quad \mathcal{C}_{\psi 3} \;\right],\; \mathcal{D} \;=\; \frac{1}{\beta}\Delta^{-2} \left[\; -\partial_y \quad \mathrm{j} k_x \;\right],$$

$$\mathcal{C}_{\psi 1} = \frac{(1-\beta)}{\beta}\Delta^{-2} \left(2\, k_x^2\, \Delta - \frac{2}{We}\mathrm{j} k_x\, \Delta\, \partial_y - \frac{1}{We^2}\Delta^2\right),$$

$$\mathcal{C}_{\psi 2} = \frac{(1-\beta)}{\beta}\Delta^{-2} \left(2\, k_x^2\, \Delta \;-\; \frac{2}{We}\mathrm{j} k_x\, \Delta\, \partial_y\right),$$

$$\mathcal{C}_{\psi 3} = \frac{(1-\beta)}{\beta} 2\, k_x^2\, \Delta^{-2}\, \Delta.$$

Here, I represents the identity operator. We note that the response of the polymer stresses $\boldsymbol{\phi}$ can be determined from the dynamics of $\boldsymbol{\xi}$ using (10) and (11). The state-space representation (12) in conjunction with (10) and (11) completely captures the dynamics of flow fluctuations in system (2). We further note that the states, $\boldsymbol{\xi}$, belong to the same Hilbert space (6) as the stream function ψ. In the next section, we show how to transform (12) into a standard singularly perturbed form. We then use singular perturbation techniques to determine the slow-fast decomposition of a channel flow of viscoelastic fluids in the absence of inertia.

IV. Singular perturbation analysis of the 2D inertialess channel flow

In this section, we show how to decompose the evolution model (12) into slow and fast subsystems. This is accomplished by bringing (12) into a standard singularly perturbed form. Furthermore, we show analytically that the fast subsystem captures the essential features of the input-output responses.

A. Singularly perturbed form of the evolution model

System (12) can be reformulated into a standard singularly perturbed form by multiplying $\boldsymbol{\xi}$ with We^2

$$\mathbf{x} \;=\; \begin{bmatrix} x_1 \\ x_2 \end{bmatrix} \;=\; We^2 \begin{bmatrix} \xi_2 \\ \xi_3 \end{bmatrix},\; z \;=\; We^2\, \xi_1,$$

and by re-scaling time with We

$$\tau \;=\; We\, t \;\Rightarrow\; \frac{\partial}{\partial t}(\cdot) \;=\; We\, \frac{\partial}{\partial \tau}(\cdot) \;=\; \frac{1}{\epsilon}\frac{\partial}{\partial \tau}(\cdot).$$

Here, we note that τ represents the new time coordinate which should not be confused with polymer stress fluctuations τ_{ij}, which are characterized with double indices. Using state variables $(\mathbf{x}, z)$ and time τ, system (12) along with (10)

and (11) can be represented by

$$\begin{bmatrix} \mathbf{x}_\tau \\ \epsilon\, z_\tau \end{bmatrix} = \begin{bmatrix} \mathcal{A}_{11}(\epsilon) & \mathcal{A}_{12}(\epsilon) \\ \mathcal{A}_{21}(\epsilon) & \mathcal{A}_{22}(\epsilon) \end{bmatrix} \begin{bmatrix} \mathbf{x} \\ z \end{bmatrix} + \begin{bmatrix} 0 \\ \mathcal{D} \end{bmatrix} \mathbf{d}, \tag{13a}$$

$$\psi = \begin{bmatrix} \mathcal{C}_{\psi\mathbf{x}}(\epsilon) & \mathcal{C}_{\psi z}(\epsilon) \end{bmatrix} \begin{bmatrix} \mathbf{x} \\ z \end{bmatrix} + \mathcal{D}\,\mathbf{d}, \tag{13b}$$

$$\boldsymbol{\phi} = \begin{bmatrix} \mathcal{C}_{\phi\mathbf{x}}(\epsilon) & \mathcal{C}_{\phi z}(\epsilon) \end{bmatrix} \begin{bmatrix} \mathbf{x} \\ z \end{bmatrix}. \tag{13c}$$

Here,

$$\epsilon = 1/We,$$

is a small positive scalar that will be used as a perturbation parameter, the τ-subscript denotes the partial derivative with respect to τ, and the operators in (13) are given in Appendix A. Since the time derivative of z is multiplied by a small positive parameter ϵ in (13a) and since the operator $\mathcal{A}_{22}$ is invertible at $\epsilon = 0$, system (13) is in a standard singularly perturbed form [12] with homogenous Dirichlet and Neumann boundary conditions on $\mathbf{x}$, z, and ψ.

B. Block-diagonal form: slow-fast decomposition of the evolution model

In this section, we demonstrate how to decompose (13) into its slow and fast subsystems. This is accomplished by first introducing a change of variables

$$\eta = z + \mathcal{L}(\epsilon)\,\mathbf{x},$$

to bring (13a) into an upper-triangular form

$$\begin{bmatrix} \mathbf{x}_\tau \\ \epsilon\,\eta_\tau \end{bmatrix} = \begin{bmatrix} \mathcal{A}_{11} - \mathcal{A}_{12}\,\mathcal{L} & \mathcal{A}_{12} \\ 0 & \mathcal{A}_{22} + \epsilon\,\mathcal{L}\,\mathcal{A}_{12} \end{bmatrix} \begin{bmatrix} \mathbf{x} \\ \eta \end{bmatrix} + \begin{bmatrix} 0 \\ \mathcal{D} \end{bmatrix} \mathbf{d}. \tag{14}$$

Here, the operator $\mathcal{L}(\epsilon)$ satisfies the following *slow-manifold* condition

$$\mathcal{A}_{21} - \mathcal{A}_{22}\,\mathcal{L} + \epsilon\,\mathcal{L}\,\mathcal{A}_{11} - \epsilon\,\mathcal{L}\,\mathcal{A}_{12}\,\mathcal{L} = 0. \tag{15}$$

Following [12], we next introduce another change of variables

$$\boldsymbol{\varphi} = \mathbf{x} - \epsilon\,\mathcal{Q}(\epsilon)\,\eta,$$

with $\mathcal{Q}$ satisfying

$$\epsilon\,(\mathcal{A}_{11} - \mathcal{A}_{12}\,\mathcal{L})\,\mathcal{Q} - \mathcal{Q}\,(\mathcal{A}_{22} + \epsilon\,\mathcal{L}\,\mathcal{A}_{12}) + \mathcal{A}_{12} = 0. \tag{16}$$

This transforms (14) into a block-diagonal form

$$\begin{bmatrix} \boldsymbol{\varphi}_\tau \\ \epsilon\,\eta_\tau \end{bmatrix} = \begin{bmatrix} \mathcal{A}_s(\epsilon) & 0 \\ 0 & \mathcal{A}_f(\epsilon) \end{bmatrix} \begin{bmatrix} \boldsymbol{\varphi} \\ \eta \end{bmatrix} + \begin{bmatrix} \mathcal{B}_s(\epsilon) \\ \mathcal{B}_f(\epsilon) \end{bmatrix} \mathbf{d}, \tag{17a}$$

$$\psi = \begin{bmatrix} \mathcal{C}_{\psi s}(\epsilon) & \mathcal{C}_{\psi f}(\epsilon) \end{bmatrix} \begin{bmatrix} \boldsymbol{\varphi} \\ \eta \end{bmatrix} + \mathcal{D}\,\mathbf{d}, \tag{17b}$$

$$\boldsymbol{\phi} = \begin{bmatrix} \mathcal{C}_{\phi s}(\epsilon) & \mathcal{C}_{\phi f}(\epsilon) \end{bmatrix} \begin{bmatrix} \boldsymbol{\varphi} \\ \eta \end{bmatrix}, \tag{17c}$$

where

$$\begin{aligned} \mathcal{A}_s &= \mathcal{A}_{11} - \mathcal{A}_{12}\,\mathcal{L}, & \mathcal{A}_f &= \mathcal{A}_{22} + \epsilon\,\mathcal{L}\,\mathcal{A}_{12}, \\ \mathcal{B}_s &= -\mathcal{Q}\,\mathcal{D}, & \mathcal{B}_f &= \mathcal{D}, \\ \mathcal{C}_{\psi s} &= \mathcal{C}_{\psi\mathbf{x}} - \mathcal{C}_{\psi z}\,\mathcal{L}, & \mathcal{C}_{\psi f} &= \mathcal{C}_{\psi z} + \epsilon\,(\mathcal{C}_{\psi\mathbf{x}} - \mathcal{C}_{\psi z}\,\mathcal{L})\,\mathcal{Q}, \\ \mathcal{C}_{\phi s} &= \mathcal{C}_{\phi\mathbf{x}} - \mathcal{C}_{\phi z}\,\mathcal{L}, & \mathcal{C}_{\phi f} &= \mathcal{C}_{\phi z} + \epsilon\,(\mathcal{C}_{\phi\mathbf{x}} - \mathcal{C}_{\phi z}\,\mathcal{L})\,\mathcal{Q}. \end{aligned}$$

Since the operators in (13) depend on the parameter ϵ, we next employ a perturbation analysis of (15) and (16) to determine the operators $\mathcal{L}$ and $\mathcal{Q}$. By substituting the following representations of the operators $\mathcal{L}$ and $\mathcal{Q}$

$$\mathcal{L}(\epsilon) = \sum_{i=0}^{\infty} \epsilon^i\,\mathcal{L}_i, \quad \mathcal{Q}(\epsilon) = \sum_{i=0}^{\infty} \epsilon^i\,\mathcal{Q}_i, \tag{18}$$

into (15) and (16), and by equating terms of equal order in ϵ (see Appendix A) we obtain

$$\mathcal{O}(\epsilon^0): \quad \mathcal{L}_0 = \begin{bmatrix} I & I \end{bmatrix}, \ \mathcal{Q}_0 = \begin{bmatrix} 0 & 0 \end{bmatrix}^T, \tag{19a}$$

$$\mathcal{O}(\epsilon^1): \begin{cases} \mathcal{L}_1 = \left(\mathcal{C}^0_{\psi 1}\right)^{-1} \begin{bmatrix} 0 & -\mathcal{C}^1_{\psi 1} \end{bmatrix}, \\ \mathcal{Q}_1 = \begin{bmatrix} (\mathcal{C}^0_{\psi 1})^{-1} & 0 \end{bmatrix}^T. \end{cases} \tag{19b}$$

The higher order terms in ϵ are not reported here for brevity. In the next section, we analyze the slow and fast subsystems in (17).

C. Analysis of slow and fast subsystems

In this section, we conduct analysis of the slow and fast subsystems of (17). The detailed derivations are given in Appendix A. We show that, for large value of the Weissenberg number, the dynamics of flow fluctuations are captured by the response of the fast subsystem with state η.

Utilizing the expansions of $\mathcal{L}$ and $\mathcal{Q}$ in (18), the solutions $\boldsymbol{\varphi}$ and η are determined by applying the temporal Fourier transform to (17a) with zero initial conditions

$$\boldsymbol{\varphi} = \epsilon\,(\mathrm{j}\Omega I - \mathcal{A}_s(\epsilon))^{-1}\,(\mathcal{B}_{s1} + \epsilon\,\mathcal{B}_{s2} + \ldots)\,\mathbf{d} = \epsilon\,\mathcal{H}_s\,\mathbf{d}, \tag{20a}$$

$$\eta = (\mathrm{j}\Omega\epsilon I - \mathcal{A}_f(\epsilon))^{-1}\,\mathcal{B}_f\,\mathbf{d} = \mathcal{H}_f\,\mathbf{d}, \tag{20b}$$

where Ω is the temporal frequency corresponding to the time variable τ. Here, for a fixed temporal frequency Ω, $\mathcal{H}_s$ and $\mathcal{H}_f$ are operators in y, mapping the forcing $\mathbf{d}$ to the responses of the slow ($\boldsymbol{\varphi}$) and fast (η) subsystems. Furthermore, since

$$\begin{aligned} \mathcal{C}_{\psi s}(\epsilon) &= \epsilon^2\,\mathcal{C}_{\psi s,2} + \epsilon^3\,\mathcal{C}_{\psi s,3} + \mathcal{O}(\epsilon^4), \\ \mathcal{C}_{\psi f}(\epsilon) &= \mathcal{C}_{\psi f,0} + \epsilon\,\mathcal{C}_{\psi f,1} + \mathcal{O}(\epsilon^2), \\ \mathcal{C}_{\phi s}(\epsilon) &= \mathcal{C}_{\phi s,0} + \epsilon\,\mathcal{C}_{\phi s,1} + \mathcal{O}(\epsilon^2), \\ \mathcal{C}_{\phi f}(\epsilon) &= \mathcal{C}_{\phi f,0} + \epsilon\,\mathcal{C}_{\phi f,1} + \mathcal{O}(\epsilon^2), \end{aligned}$$

the responses of the stream function ψ and polymer stresses $\boldsymbol{\phi}$ can be obtained by substituting (20a) and (20b) into the

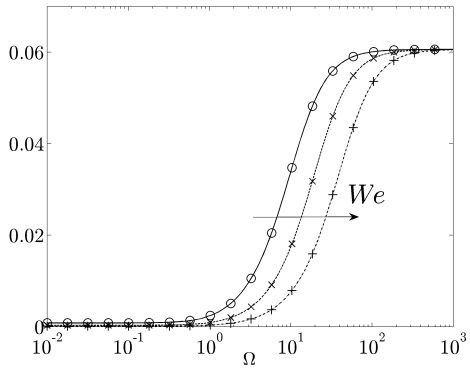

Fig. 2. The temporal frequency dependence of $\Pi_{\psi f}$ and Π_{ψ} in flows with $k_x = 1$, $\beta = 0.5$, and $\epsilon = \{0.02, 1 \times 10^{-2}, 5 \times 10^{-3}\}$. The lines represent the results for Π_{ψ}. The symbols represent the results for $\Pi_{\psi f}$ which is the response from only the fast system.

temporal Fourier transforms of (17b) and (17c)

$$\begin{aligned}\psi \;&=\; \epsilon^3 \left(\mathcal{C}_{\psi s,2} + \epsilon\, \mathcal{C}_{\psi s,3} + \ldots\right) \left(\mathrm{j}\Omega I - \mathcal{A}_s(\epsilon)\right)^{-1} && \text{(21a)}\\ &\quad\times \left(\mathcal{B}_{s1} + \epsilon\, \mathcal{B}_{s2} + \ldots\right) \mathbf{d} \;+\; \Big\{ \left(\mathcal{C}_{\psi f,0} + \epsilon\, \mathcal{C}_{\psi f,1} + \ldots\right)\\ &\quad\times \left(\mathrm{j}\Omega\epsilon I - \mathcal{A}_f(\epsilon)\right)^{-1} \mathcal{B}_f + \mathcal{D} \Big\}\, \mathbf{d},\\ &=\; \left(\epsilon^3\, \mathcal{H}_{\psi s} \;+\; \mathcal{H}_{\psi f}\right) \mathbf{d} \;=\; \mathcal{H}_{\psi} \mathbf{d}, && \text{(21b)}\\ \boldsymbol{\phi} \;&=\; \epsilon \left(\mathcal{C}_{\phi s,0} + \epsilon\, \mathcal{C}_{\phi s,1} + \ldots\right) \left(\mathrm{j}\Omega I - \mathcal{A}_s(\epsilon)\right)^{-1} && \text{(21c)}\\ &\quad\times \left(\mathcal{B}_{s1} + \epsilon\, \mathcal{B}_{s2} + \ldots\right) \mathbf{d}\\ &\quad+\; \left(\mathcal{C}_{\phi f,0} + \epsilon\, \mathcal{C}_{\phi f,1} + \ldots\right) \left(\mathrm{j}\Omega\epsilon I - \mathcal{A}_f(\epsilon)\right)^{-1} \mathcal{B}_f\, \mathbf{d},\\ &=\; \left(\epsilon\, \mathcal{H}_{\phi s} \;+\; \mathcal{H}_{\phi f}\right) \mathbf{d} \;=\; \mathcal{H}_{\phi} \mathbf{d}. && \text{(21d)}\end{aligned}$$

The frequency response operators $\{\mathcal{H}_{ij}\}$ in (21b) and (21d) map the forcing $\mathbf{d}$ to the stream function $(i = \psi)$ and polymer stresses $(i = \phi)$ with $\{j = s, f\}$ identifying the contributions from the slow and fast subsystems, respectively.

It is clear from (21) that, in high Weissenberg number regime, the response of the slow subsystem has negligible influence on the stream function and the polymer stresses. This illustrates that the fast subsystem has the largest influence on the system's response.

V. Frequency responses of a 2D inertialess flow of viscoelastic fluids

Here, we compute the frequency responses of the inertialess flow of viscoelastic fluids using the slow-fast decomposition (17). In particular, we are interested in computing the power spectral density for the 2D inertialess flow. For a fixed temporal frequency Ω, this quantity is determined by the Hilbert-Schmidt norm of the frequency response operator $\mathcal{H}_{ij}$,

$$\Pi_{ij}(\Omega) = \|\mathcal{H}_{ij}(\Omega)\|^2_{HS} = \text{trace}\left(\mathcal{H}_{ij}(\Omega)\, \mathcal{H}^{\star}_{ij}(\Omega)\right),$$

where $\mathcal{H}^{\star}_{ij}$ represents the adjoint of the operator $\mathcal{H}_{ij}$. All computations are done using a pseudo-spectral method [13]. Convergence of the results is tested by doubling the number of collocation points.

In view of page limitations, we will only consider the response of the velocity fluctuations. These can be determined by analyzing the frequency response operator (21b). Figure 2 shows the Hilbert-Schmidt norm of the frequency response operator from forcing to the stream function, i.e., $\Pi_{\psi f}$ and Π_{ψ}. Note that the power spectral density as a function of Ω for the stream function has a high-pass characteristic. This response is a consequence of the direct feed-through term from the forcing to the stream function. In addition, the increase in We (decrease in ϵ) moves the cut-off frequency to higher values of Ω. We further note that $\Pi_{\psi f}$ lies on top of Π_{ψ} which indicates that at high Weissenberg numbers the fast subsystem reliably captures the response of the entire system. This thus verifies the predictions obtained using perturbation analysis.

VI. Concluding remarks

We study the frequency responses of a two-dimensional inertialess shear-driven flow of viscoelastic fluids. In particular, we have shown that the dynamics can be decomposed into slow and fast subsystems. This is accomplished by rewriting the evolution equations in terms of low-pass filtered versions of the stream function. This state-space representation admits a standard singularly perturbed form, which is obtained by rescaling time with the Weissenberg number. We then show analytically that the dynamics of flow fluctuations can be captured by the response of the fast subsystem. This demonstrates that the inertialess shear-driven flow of strongly elastic fluids can be modeled by only a single PDE instead of the original system of three PDEs (which are determined by constitutive equation for polymer stresses). Furthermore, this new formulation does not inherit any numerical instabilities from the original model.

Our ongoing effort is devoted to studying the full nonlinear equations using singular perturbation methods. Successful analysis of the nonlinear equations may identify new methods for simulating full three-dimensional flows, thereby leading to new ways of studying the intriguing phenomenon of 'elastic turbulence' [1]–[3] in wall-bounded shear flows of viscoelastic fluids.

Appendix

A. System operators

In this section, we present the system operators used in each section of the paper.

1) Section III: The operators $\mathcal{C}_{\psi i}$ for $\{i = 1, 2, 3\}$ in (12) are given by

$$\begin{aligned}\mathcal{C}_{\psi 1}(\epsilon) \;&=\; \mathcal{C}_{\psi 1,0} \;+\; \epsilon\, \mathcal{C}_{\psi 1,1} \;+\; \epsilon^2\, \mathcal{C}_{\psi 1,2},\\ \mathcal{C}_{\psi 2}(\epsilon) \;&=\; \mathcal{C}_{\psi 2,0} \;+\; \epsilon\, \mathcal{C}_{\psi 2,1}, \quad \mathcal{C}_{\psi 3}(\epsilon) \;=\; \mathcal{C}_{\psi 3,0},\end{aligned}$$

where

$$\begin{aligned}\mathcal{C}_{\psi 1,0} \;&=\; \mathcal{C}_{\psi 2,0} \;=\; \mathcal{C}_{\psi 3,0} \;=\; \frac{(1-\beta)}{\beta} 2\, k_x^2\, \Delta^{-2}\, \Delta,\\ \mathcal{C}_{\psi 1,1} \;&=\; \mathcal{C}_{\psi 2,1} \;=\; -\frac{(1-\beta)}{\beta} 2\, \mathrm{j} k_x\, \Delta^{-2}\, \Delta\, \partial_y,\\ \mathcal{C}_{\psi 1,2} \;&=\; -\frac{(1-\beta)}{\beta}.\end{aligned}$$

2) Section IV: The operators in (13) are given by

$$\mathcal{A}_{11} = \begin{bmatrix} -(\epsilon + \mathrm{j}k_x\, y) & 0 \\ \epsilon & -(\epsilon + \mathrm{j}k_x\, y) \end{bmatrix},$$

$$\mathcal{A}_{12} = \begin{bmatrix} \epsilon \\ 0 \end{bmatrix},\ \mathcal{A}_{21} = \mathcal{C}_{\psi\mathbf{x}} = \begin{bmatrix} \mathcal{C}_{\psi 2} & \mathcal{C}_{\psi 3} \end{bmatrix},$$

$$\mathcal{A}_{22} = \mathcal{C}_{\psi 1} - \left(\epsilon^2 + \epsilon\, \mathrm{j}k_x\, y\right),\ \mathcal{C}_{\psi z} = \mathcal{C}_{\psi 1},$$

$$\mathcal{C}_{\phi\mathbf{x}} = \begin{bmatrix} \mathcal{C}_{12} & 0 \\ \mathcal{C}_{22} & \mathcal{C}_{23} \\ \mathcal{C}_{32} & \mathcal{C}_{33} \end{bmatrix},\ \mathcal{C}_{\phi z} = \begin{bmatrix} \mathcal{C}_{11} \\ \mathcal{C}_{21} \\ \mathcal{C}_{31} \end{bmatrix}.$$

where

$$\begin{aligned}
\mathcal{C}_{11} &= 2\,\epsilon\, k_x^2 - 2\,\epsilon^2\, \mathrm{j}k_x\, \partial_y = \epsilon\, \mathcal{C}_{11,1} + \epsilon^2\, \mathcal{C}_{11,2}, \\
\mathcal{C}_{12} &= 2\,\epsilon\, k_x^2 = \epsilon\, \mathcal{C}_{12,1}, \\
\mathcal{C}_{21} &= 2\, k_x^2 + \epsilon^2 \left(\partial_{yy} + k_x^2\right) = \mathcal{C}_{21,0} + \epsilon^2\, \mathcal{C}_{21,2}, \\
\mathcal{C}_{22} &= 2\, k_x^2 = \mathcal{C}_{22,0},\ \mathcal{C}_{23} = 2\, k_x^2 = \mathcal{C}_{23,0}, \\
\mathcal{C}_{31} &= 4\, \mathrm{j}k_x\, \partial_y + 2\,\epsilon\, \partial_{yy} + 2\,\epsilon^2\, \mathrm{j}k_x\, \partial_y \\
&= \mathcal{C}_{31,0} + \epsilon\, \mathcal{C}_{31,1} + \epsilon^2\, \mathcal{C}_{31,2}, \\
\mathcal{C}_{32} &= 4\, \mathrm{j}k_x\, \partial_y + 2\,\epsilon\, \partial_{yy} = \mathcal{C}_{32,0} + \epsilon\, \mathcal{C}_{32,1}, \\
\mathcal{C}_{33} &= 4\, \mathrm{j}k_x\, \partial_y = \mathcal{C}_{33,0}.
\end{aligned}$$

Furthermore, we note that each operator in (13) can be factorized in terms of ϵ, e.g.,

$$\begin{aligned}
\mathcal{A}_{11}(\epsilon) &= \begin{bmatrix} -(\epsilon + \mathrm{j}k_x\, y) & 0 \\ \epsilon & -(\epsilon + \mathrm{j}k_x\, y) \end{bmatrix} \\
&= \underbrace{\begin{bmatrix} -\mathrm{j}k_x\, y & 0 \\ 0 & -\mathrm{j}k_x\, y \end{bmatrix}}_{\mathcal{A}_{11,0}} + \epsilon \underbrace{\begin{bmatrix} -I & 0 \\ I & -I \end{bmatrix}}_{\mathcal{A}_{11,1}}.
\end{aligned}$$

We employ a perturbation analysis of (15) and (16) to determine the operators $\mathcal{L}$ and $\mathcal{Q}$ with ϵ being the perturbation parameter. This is done by substituting (18) into (15) and (16) and equating terms of equal order in ϵ, which yields

$$\mathcal{O}(\epsilon^0): \begin{cases} \mathcal{L}_0 = \left(\mathcal{A}_{22}^0\right)^{-1} \mathcal{A}_{21}^0 = \left(\mathcal{C}_{\psi 1}^0\right)^{-1} \begin{bmatrix} \mathcal{C}_{\psi 2}^0 & \mathcal{C}_{\psi 3}^0 \end{bmatrix} \\ \quad = \begin{bmatrix} I & I \end{bmatrix}, \\ \mathcal{Q}_0 = \mathcal{A}_{12}^0 \left(\mathcal{A}_{22}^0\right)^{-1} = \begin{bmatrix} 0 & 0 \end{bmatrix}^T, \end{cases}$$

$$\mathcal{O}(\epsilon^1): \begin{cases} \mathcal{L}_1 = \left(\mathcal{A}_{22}^0\right)^{-1} \left(\mathcal{A}_{21}^1 - \mathcal{A}_{22}^1 \mathcal{L}_0 + \mathcal{L}_0 \mathcal{A}_{11}^0\right) \\ \quad = \left(\mathcal{C}_{\psi 1}^0\right)^{-1} \begin{bmatrix} 0 & -\mathcal{C}_{\psi 1}^1 \end{bmatrix}, \\ \mathcal{Q}_1 = \mathcal{A}_{12}^1 \left(\mathcal{A}_{22}^0\right)^{-1} = \begin{bmatrix} (\mathcal{C}_{\psi 1}^0)^{-1} & 0 \end{bmatrix}^T. \end{cases}$$

Using the expansions for the operators $\mathcal{L}$ and $\mathcal{Q}$, the operators in (17) are given by

$$\begin{aligned}
\mathcal{A}_s(\epsilon) &= \mathcal{A}_{11}(\epsilon) - \mathcal{A}_{12}(\epsilon)\, \mathcal{L}(\epsilon) = \mathcal{A}_{11,0} \\
&\quad + \epsilon \left(\mathcal{A}_{11,1} - \mathcal{A}_{12,1}\, \mathcal{L}_0\right) - \epsilon^2\, \mathcal{A}_{12,1}\, \mathcal{L}_1 + \mathcal{O}(\epsilon^3) \\
&= \mathcal{A}_{s0} + \epsilon\, \mathcal{A}_{s1} + \epsilon^2\, \mathcal{A}_{s2} + \mathcal{O}(\epsilon^3), \\
\mathcal{A}_f(\epsilon) &= \mathcal{A}_{22}(\epsilon) + \epsilon\, \mathcal{L}(\epsilon)\, \mathcal{A}_{12}(\epsilon) = \mathcal{A}_{22,0} + \epsilon \mathcal{A}_{22,1} \\
&\quad + \epsilon^2 \left(\mathcal{A}_{22,2} + \mathcal{L}_0\, \mathcal{A}_{12,1}\right) + \mathcal{O}(\epsilon^3) \\
&= \mathcal{A}_{f0} + \epsilon\, \mathcal{A}_{f1} + \epsilon^2\, \mathcal{A}_{f2} + \mathcal{O}(\epsilon^3),
\end{aligned}$$

$$\begin{aligned}
\mathcal{B}_s(\epsilon) &= -\mathcal{Q}(\epsilon)\mathcal{D} = -\left(\mathcal{Q}_0 + \epsilon \mathcal{Q}_1\right)\mathcal{D} + \mathcal{O}(\epsilon^3) \\
&= -\epsilon\, \mathcal{Q}_1\, \mathcal{D} + \mathcal{O}(\epsilon^3) = \mathcal{B}_{s1} + \mathcal{O}(\epsilon^3), \\
\mathcal{B}_f(\epsilon) &= \mathcal{D} = \mathcal{B}_{f0}, \\
\mathcal{C}_{\psi s}(\epsilon) &= \mathcal{C}_{\psi\mathbf{x}}(\epsilon) - \mathcal{C}_{\psi z}(\epsilon)\, \mathcal{L}(\epsilon) = \left(\mathcal{C}_{\psi\mathbf{x},0} - \mathcal{C}_{\psi 1,0}\mathcal{L}_0\right) \\
&\quad + \epsilon \left(\mathcal{C}_{\psi\mathbf{x},1} - \mathcal{C}_{\psi 1,0}\, \mathcal{L}_1 - \mathcal{C}_{\psi 1,1}\, \mathcal{L}_0\right) \\
&\quad - \epsilon^2 \left(\mathcal{C}_{\psi 1,0}\, \mathcal{L}_2 + \mathcal{C}_{\psi 1,1}\, \mathcal{L}_1 + \mathcal{C}_{\psi 2,1}\, \mathcal{L}_0\right) + \mathcal{O}(\epsilon^3) \\
&= \mathcal{C}_{\psi s,0} + \epsilon\, \mathcal{C}_{\psi s,1} + \epsilon^2\, \mathcal{C}_{\psi s,2} + \mathcal{O}(\epsilon^3), \\
\mathcal{C}_{\psi f}(\epsilon) &= \mathcal{C}_{\psi z}(\epsilon) + \epsilon \left(\mathcal{C}_{\psi\mathbf{x}}(\epsilon) - \mathcal{C}_{\psi z}(\epsilon)\, \mathcal{L}(\epsilon)\right) \mathcal{Q}(\epsilon) \\
&= \mathcal{C}_{\psi 1,0} + \epsilon\, \mathcal{C}_{\psi 1,1} \\
&\quad + \epsilon^2 \left(\mathcal{C}_{\psi\mathbf{x},0} - \mathcal{C}_{\psi 1,0}\, \mathcal{L}_0\right) \mathcal{Q}_1 + \mathcal{O}(\epsilon^3) \\
&= \mathcal{C}_{\psi f,0} + \epsilon\, \mathcal{C}_{\psi f,1} + \epsilon^2\, \mathcal{C}_{\psi f,2} + \mathcal{O}(\epsilon^3).
\end{aligned}$$

Since

$$\begin{aligned}
\mathcal{C}_{\psi\mathbf{x},0} - \mathcal{C}_{\psi 1,0}\, \mathcal{L}_0 &= \begin{bmatrix} \mathcal{C}_{\psi 2,0} & \mathcal{C}_{\psi 3,0} \end{bmatrix} - \mathcal{C}_{\psi 1,0} \begin{bmatrix} I & I \end{bmatrix} \\
&= \begin{bmatrix} 0 & 0 \end{bmatrix},
\end{aligned}$$

and

$$\begin{aligned}
\mathcal{C}_{\psi\mathbf{x},1} - \mathcal{C}_{\psi 1,1} - \mathcal{C}_{\psi 1,0}\, \mathcal{L}_1 \mathcal{L}_0 &= \begin{bmatrix} \mathcal{C}_{\psi 2,1} & 0 \end{bmatrix} - \mathcal{C}_{\psi 1,1} \begin{bmatrix} I & I \end{bmatrix} \\
&\quad - \mathcal{C}_{\psi 1,0} \left(\mathcal{C}_{\psi 1,0}\right)^{-1} \begin{bmatrix} 0 & -\mathcal{C}_{\psi 1,1} \end{bmatrix} \\
&= \begin{bmatrix} 0 & 0 \end{bmatrix},
\end{aligned}$$

operator $\mathcal{C}_{\psi s}$ can be simplified to

$$\mathcal{C}_{\psi s}(\epsilon) = \epsilon^2\, \mathcal{C}_{\psi s,2} + \mathcal{O}(\epsilon^3).$$

REFERENCES

[1] R. G. Larson, "Turbulence without inertia," *Nature*, vol. 405, pp. 27–28, 2000.

[2] A. Groisman and V. Steinberg, "Elastic turbulence in a polymer solution flow," *Nature*, vol. 405, pp. 53–55, 2000.

[3] A. Groisman and V. Steinberg, "Efficient mixing at low reynolds numbers using polymer additives," *Nature*, vol. 410, pp. 905–908, 2001.

[4] N. Hoda, M. R. Jovanović, and S. Kumar, "Energy amplification in channel flows of viscoelastic fluids," *J. Fluid Mech.*, vol. 601, pp. 407–424, April 2008.

[5] N. Hoda, M. R. Jovanović, and S. Kumar, "Frequency responses of streamwise-constant perturbations in channel flows of Oldroyd-B fluids," *J. Fluid Mech.*, vol. 625, pp. 411–434, April 2009.

[6] M. R. Jovanović and S. Kumar, "Transient growth without inertia," *Phys. Fluids*, vol. 22, no. 2, p. 023101, February 2010.

[7] M. R. Jovanović and S. Kumar, "Nonmodal amplification of stochastic disturbances in strongly elastic channel flows," *J. Non-Newtonian Fluid Mech.*, vol. 166, no. 14-15, pp. 755–778, August 2011.

[8] B. K. Lieu, M. R. Jovanovic, and S. Kumar, "Worst-case amplification of disturbances in inertialess flows of viscoelastic fluids," in *Preprints of the 18th IFAC World Congress*, Milano, Italy, 2011, pp. 14 458–14 463.

[9] R. Kupferman, "On the linear stability of plane Couette flow for an Oldroyd-B fluid and its numerical approximation," *J. Non-Newtonian Fluid Mech.*, vol. 127, no. 2-3, pp. 169–190, 2005.

[10] M. D. Graham, "Effect of axial flow on viscoelastic Taylor-Couette instability," *J. Fluid Mech.*, vol. 360, no. 1, pp. 341–374, 1998.

[11] R. G. Larson, *The Structure and Rheology of Complex Fluids*. Oxford University Press, 1999.

[12] P. V. Kokotović, H. K. Khalil, and J. O'Reilly, *Singular Perturbation Methods in Control: Analysis and Design*. SIAM, 1999, vol. 25.

[13] J. A. C. Weideman and S. C. Reddy, "A MATLAB differentiation matrix suite," *ACM T. Math. Software*, vol. 26, no. 4, pp. 465–519, 2000.